



Influence of pyrolysis temperature on sludge biochar: the ecological risk assessment of heavy metals and the adsorption of Cd(II)

Menglan Wu¹ · Bo Liu¹ · Jun Li¹ · Xintai Su^{1,2} · Weizhen Liu^{1,2} · Xiaoqin Li^{1,2}

Received: 22 June 2022 / Accepted: 28 August 2022 / Published online: 16 September 2022
© The Author(s), under exclusive licence to Springer-Verlag GmbH Germany, part of Springer Nature 2022

Abstract

Pyrolysis of sludge to biochar can not only reduce the sludge volume, toxic organic compound, and pathogens, but also be applied as effective adsorbents. However, the immobilization of heavy metals in the sludge and the properties of the biochar greatly rely on the pyrolysis temperature. In this paper, municipal sludge biochar (SBC) was prepared from 400 to 1000 °C. Pyrolysis immobilized heavy metals in sludge and the potential ecological risk of heavy metals significantly decreased to low level at temperature above 500 °C. At 700 °C, the adsorption capacity of Cd(II) reached a maximum (120.24 mg·g⁻¹). The Cd(II) adsorption fitted the Pseudo-second-order model, indicating the existence of chemical adsorption. The adsorption capacity increased along with the initial pH and slowed down after pH reached 5.5. The existence of coexisting cations (Ca²⁺ and Na⁺) and anions (SO₄²⁻ and NO₃⁻) displayed different degree of inhibitory action on Cd(II) adsorption. The SEM, XRD, FTIR, and XPS analysis of sludge biochar before and after adsorption revealed that there were CdCO₃, CdSO₄, Cd₂SiO₄, Cd₃(PO₄)₂, and Cd₉(PO₄)₆ appearing on the surface of sludge biochar, suggesting that the adsorption of Cd(II) by SBC included co-precipitation, ion exchange, coordination with π electrons, and complexation. It was confirmed that different properties formed by pyrolysis temperature made a difference in adsorption mechanism of sludge biochar.

Keywords Sludge biochar · Pyrolysis temperature · Cd(II) · Heavy metal immobilization · Adsorption mechanism

Introduction

Cadmium (Cd) is a highly mobile heavy metal with known carcinogenic toxicity. Due to the discharge from mining, electroplating, battery industry, dye, etc., the contamination of Cd in the environment is very severe in China (Huang et al. 2017). At present, the methods to remove Cd(II) from wastewater mainly include chemical precipitation, electrochemical treatment, membrane filtration, ion exchange, and adsorption (Carolin et al. 2017), among which adsorption is

one of the most promising due to its advantages of low cost, high efficiency, and easy recovery (Wu et al. 2021). Common sorbents include activated carbon, ion exchange resin, chitosan, zeolite (Li et al. 2018b), and clay (Gu et al. 2018). Biochar is a carbon enriched pyrolysis product obtained from biomasses such as livestock manure and crops. Due to its favorable pore structure, large specific surface area, and abundant functional groups, biochar has also been applied for the adsorption of Cd(II) (Wang et al. 2020). The adsorption capacity of biochar on Cd(II) is nearly three times that of activated carbon (Kołodziejńska et al. 2017).

On the other hand, the sludge treatment and disposal has been a global concern in the past decades. In 2020, the production of municipal sludge (moisture content based on 80%) in China and EU countries reached 90 and 400 million tons, respectively (Li et al. 2021). Pyrolysis of sludge to biochar can not only greatly reduce the sludge volume, the toxic organic compounds and pathogens, but also immobilize heavy metals such as Cr, Zn, and Pb in the sludge (Zhang et al. 2020a; Xiong et al. 2021). Previous studies showed that the sludge biochar (SBC) can effectively adsorb Cd(II) through electrostatic attraction, co-precipitation, ion

Responsible Editor: Zhihong Xu

✉ Xiaoqin Li
xqli306@scut.edu.cn

¹ School of Environment and Energy, Guangdong Provincial Key Laboratory of Solid Wastes Pollution Control and Recycling, South China University of Technology, Guangzhou, Guangdong 510006, People's Republic of China

² The Key Laboratory of Pollution Control and Ecosystem Restoration in Industry Clusters of the Ministry of Education, South China University of Technology, Guangzhou 510006, People's Republic of China

exchange, and complexation (Yoon et al., 2017). The adsorption capacity of the SBC relies on the sludge source. For instance, the removal capacity of Cd(II) by biochar from sewage sludge is $97.3 \text{ mg}\cdot\text{g}^{-1}$, which is more than twice compared to that from paper mill sludge and palm oil mill sludge (Xue et al. 2019).

It is also found that pyrolysis temperature affects the properties of biochar, such as the specific surface area, pore structure, pH, and the functional groups (Zhang et al. 2020c). The specific surface area and pH values of biochar increase rapidly with the increase of pyrolysis temperature when it is less than $800 \text{ }^\circ\text{C}$ (Li et al. 2019). Zhang et al. reported that functional groups such as -OH, C-H, and C=C reduce with the increase of pyrolysis temperature (Zhang et al. 2020c). Furthermore, pyrolysis temperature also affects the mobility of the heavy metals in the biochar. For example, the chemical speciation of heavy metals transform into more stable oxidizable and residual fractions with the increase of pyrolysis temperature (Li et al. 2021). Therefore, it is important to investigate both the adsorption performance and the heavy metal immobilization when using sludge to produce biochar.

Since previous studies mainly focus on the modification of biochar to increase the adsorption capacity at a certain or several pyrolysis temperatures, in this work, sludge biochar was prepared from municipal sludge at various pyrolysis temperatures ($400\text{--}1000 \text{ }^\circ\text{C}$). The objectives are to (1) assess the effect of pyrolysis temperature on heavy metal immobilization in sludge biochar and the potential ecological risk of sludge biochar; (2) investigate the effect of pyrolysis temperature on the morphologies, structure and physicochemical properties of sludge biochar; (3) investigate the adsorption mechanism of Cd(II) by sludge biochar. Through this study, it is expected to give a thorough assessment of sludge biochar reclamation and its application in heavy metal removal.

Materials and methods

Chemical reagents

Ammonium acetate ($\text{CH}_3\text{COONH}_4$), calcium chloride (CaCl_2), sodium chloride (NaCl), and sodium hydroxide (NaOH) were purchased from Aladdin Biochemical Technology Co., Ltd (Shanghai, China). Nitric acid (HNO_3) and sodium nitrate (NaNO_3) were obtained from Chemical Reagent Factory (Guangzhou, China). Cadmium chloride anhydrous (CdCl_2) was provided by Aladdin Reagent Co., Ltd (Shanghai, China). Acetic acid (CH_3COOH) was supplied by Kemiou Chemical Reagent Co., Ltd (Tianjin, China). Hydroxylamine hydrochloride ($\text{NH}_2\text{OH}\cdot\text{HCl}$) was purchased from Maclin Biochemical Technology Co., Ltd (Shanghai, China). Hydrogen peroxide (H_2O_2) was obtained from Dongzheng Chemical glass Instrument Co., Ltd (Guangzhou,

China). Anhydrous sodium sulfate (NaSO_4) was supplied by Yongda Chemical Reagent Co., Ltd (Tianjin, China). All chemical reagents used were analytical grade and above, and deionized water obtained from deionized water system (Millipore, Elix 7, Millipore Corporation, America) was used to prepare the solution for the experiment.

Preparation of dry sewage sludge and sludge biochar

The sewage sludge (SS) used in this work was obtained from Guangzhou Haitao Environmental Protection Company, China. The SS was dried in the oven at $60 \text{ }^\circ\text{C}$, crushed and sieved through a 120-mesh stainless steel sieve, and then stored in the airtight plastic bag. The preparation of sludge biochar was conducted in an open tube furnace (Hefei Kejing Material Technology Co., Ltd, OTF-1200X). The furnace was heated to preset temperature ($400, 500, 600, 700, 800, 900,$ and $1000 \text{ }^\circ\text{C}$) at a rate of $5 \text{ }^\circ\text{C}\cdot\text{min}^{-1}$, held for 1 h and then cooled down to room temperature. N_2 was fed at a $0.5 \text{ L}\cdot\text{min}^{-1}$ flow rate during the pyrolysis and cooling process. The biochar was further crushed and sieved through a 100-mesh stainless steel sieve and stored in airtight plastic bags. Based on the pyrolysis temperature, the obtained sludge biochar was abbreviated as SBC400, SBC500, SBC600, SBC700, SBC800, SBC900, and SBC1000, respectively.

Adsorption experiments of Cd(II) by SBC

A total of 1000 ppm Cd(II) stock solution was prepared by dissolving 1.631 g CdCl_2 in 1 L deionized water and diluted to desired concentration during the batch experiments. Unless otherwise mentioned, the initial Cd(II) concentration was set at 50 ppm, SBC dosage was $0.40 \text{ g}\cdot\text{L}^{-1}$, and the liquid volume was 50 mL. The adsorption experiments were conducted in 250-mL flask at $25 \text{ }^\circ\text{C}$ and $200 \text{ r}\cdot\text{min}^{-1}$. At preset time intervals (0.25, 0.5, 0.75, 1, 3, 5, 6, 15, 24, 32, and 48 h), the supernatant was collected by passing through a $0.22\text{-}\mu\text{m}$ syringe filter and diluted with 2% HNO_3 . During the investigation of the effect of pH and coexisting ions, the reaction time was 24 h, and the pH was adjusted by 0.1 M HCl/NaOH , and Ca^{2+} , Na^+ , SO_4^{2-} , and NO_3^- concentrations were 0.02, 0.04, 0.06, 0.08, and $0.10 \text{ mol}\cdot\text{L}^{-1}$, respectively. All adsorption experiments were run in triplicate.

Heavy metal BCR fraction and potential ecological risk estimation

The heavy metals chemical states in the SS and SBC were measured according to the modified BCR sequential extraction procedure (Li et al. 2021), where heavy metals are classified into four categories according to their bioavailability from high to low: exchangeable and acid-soluble fraction

(ACE), reducible (RED), oxidizable (OXI), and residual (RES) fractions (Yuan et al. 2011). The fraction in various chemical states was further utilized to estimate the potential ecological risk index (RI) of the heavy metals based on the following equations (Wang et al., 2019; Zhao et al. 2021):

$$C_f = \frac{C_m}{C_n} \quad (1)$$

$$E_r = T_r \times C_f \quad (2)$$

$$RI = \sum E_r \quad (3)$$

where C_f is the contamination factor of individual heavy metal; C_m and C_n are the potential mobile fractions (ACE, RED, OXI) and the stable fraction (RES) of the heavy metals, respectively; E_r is the potential ecological risk factor for the individual heavy metal; T_r is the toxic factor of the individual heavy metal, which is 1, 1, 2, 5, 5 for Zn, Mn, Cr, Pb, and Pb, respectively (Jin et al. 2016). The potential risk assessment index grades of C_f , E_r , and RI are shown in Table S1.

Analytical methods

The content of C, H, O, N, and S in the sludge biochar were analyzed with an elemental analyzer (Vario EL cube, Elementar, Germany). The scanning electron microscope (EVO LS 10X-Flash6130, Zeiss, Germany) was used to detect the surface morphologies and structure of SBC500, SBC700, and SBC900. The X-ray diffractometer (Empyrean, PANalytical B.V., Netherlands) was used to analyze the crystal structure in sludge biochar before and after Cd(II) adsorption. The difference of surface functional groups was obtained using a Fourier transform infrared spectrometer (Nicolet iS5, Thermo Fisher, USA). The X-ray photoelectron spectrometer (Scientific K-Alpha, Thermo Fisher, USA) was used to analyze the phase composition of sludge biochar before and after adsorption. The concentrations of heavy metals were determined by atomic absorption spectrophotometer (AA-6300C, Shimadzu Instrument Co., Japan) or ICP-OES (Agilent, 730, USA).

Results and discussion

Effect of pyrolysis temperature on SBC's physicochemical properties

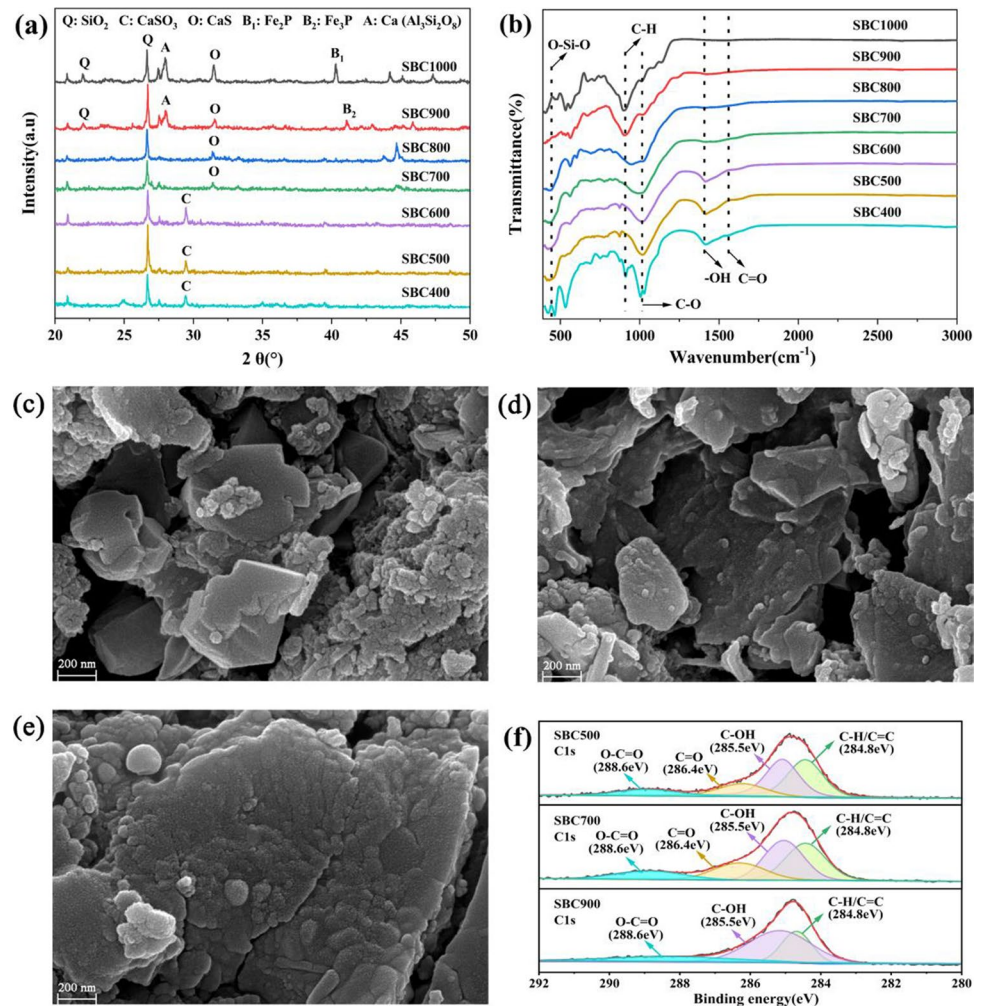
The elemental compositions of the SBC at different pyrolysis temperatures are shown in Table 1. The content of N, C, H, and O significantly decreased with the increase of pyrolysis temperature, indicating the loss of volatile organic matters (Chen et al. 2014). S content was more stable, suggesting that pyrolysis temperature had negligible effect on S. Since Cd has strong affinity towards S, the stabilized S content might enhance the adsorption of Cd and other heavy metals (Liang et al. 2020, 2021). The molar ratio of H/C, which is often used to characterize the aromaticity of SBC, increased with the increase of pyrolysis temperature, implying that the aromaticity and carbonization degree of sludge biochar increased (Jin et al. 2016). Meanwhile, the molar ratio of O/C and (O+N)/C, indicator of the hydrophilicity and polarity of SBC, decreased with the increase of the pyrolysis temperature due to the loss of oxygen-containing functional groups (Zhang et al. 2019; Gao et al. 2019).

Figure 1a shows the XRD spectrum of SBC at pyrolysis temperatures from 400 to 1000 °C. The characteristic peak at $2\theta = 26.6^\circ$ corresponded to SiO_2 , which originated from the sewage sludge. At lower pyrolysis temperatures (400–600 °C), the characteristic peak at $2\theta = 29.2^\circ$ was attributed to CaSO_3 . The peak disappeared at 700–1000 °C and a new characteristic peak corresponding to CaS at $2\theta = 31.4^\circ$ appeared, due to the reduction of S in CaSO_3 by C to CaS at higher temperature (Liu et al. 2021). At 900–1000 °C, new peaks corresponding to $\text{Ca}(\text{Al}_3\text{Si}_2\text{O}_8)$, Fe_2P , and Fe_3P appeared; these peaked might come from the flocculant during the wastewater treatment. FTIR analysis further verified the functional groups changes of SBC with pyrolysis temperature (Fig. 1b). The peak at 466 cm^{-1} corresponding to O-Si-O vibration verified the existence of SiO_2 in SBC. The peak at 866 cm^{-1} is attributed to the vibration of aromatic C-H, which provides π electrons and is conducive to the adsorption of heavy metal cations (Chen et al. 2014). The peaks at 1037 cm^{-1} , 1420 cm^{-1} , and

Table 1 Elemental compositions of SBC obtained under different pyrolysis temperatures

Sample	N (%)	C (%)	O (%)	H (%)	S (%)	H/C	O/C	(O+N)/C
SBC400	0.89	8.05	15.96	1.34	1.12	1.98	1.49	1.58
SBC500	0.68	6.84	14.63	0.76	0.82	1.32	1.61	1.69
SBC600	0.53	6.23	12.62	0.54	0.80	1.03	1.52	1.59
SBC700	0.33	4.87	9.11	0.44	0.84	1.07	1.40	1.46
SBC800	0.19	4.25	6.98	0.33	0.97	0.93	1.23	1.27
SBC900	0.08	3.21	4.21	0.20	0.99	0.75	0.98	1.01
SBC1000	0.05	2.38	2.31	0.06	1.03	0.29	0.73	0.75

Fig. 1 **a** XRD spectrum of seven sludge biochar; **b** FTIR spectrum of seven sludge biochar; SEM images of **c** SBC500, **d** SBC700, and **e** SBC900; **f** C1s XPS spectra of SBC500, SBC700, and SBC900



1615 cm^{-1} , corresponding to the vibration of C-O, -OH, and C=O, gradually weakened as the pyrolysis temperature increased. This might affect the adsorption on Cd(II) by SBC since oxygen-containing functional groups had a stronger affinity to cations (Li et al. 2017).

SBC500, SBC700, and SBC900 were further investigated by SEM and XPS. SEM images show that all of the three SBC had blocks or lamellar structure (Fig. 1c–e). The surface of SBC500 was smoother, while SBC700 was similar in size but had more flakes on the surface. With the further increase in pyrolysis temperature to 900 °C, SBC sintered and the surface roughness increased. The specific surface areas of the three SBC were $23.57\text{ m}^2\cdot\text{g}^{-1}$, $30.96\text{ m}^2\cdot\text{g}^{-1}$, and $28.33\text{ m}^2\cdot\text{g}^{-1}$, respectively. The wide scan XPS spectrum (Fig. S1) shows that the main elements in SBC were C and O. C1s XPS spectra (Fig. 1f) contained C-H/C=C, C-OH, C=O, and O-C=O bonds; C=O bond disappeared in SBC900, indicating that high pyrolysis temperature led to the decomposition of oxygen-containing functional groups. The results of XPS analysis are consistent with those of

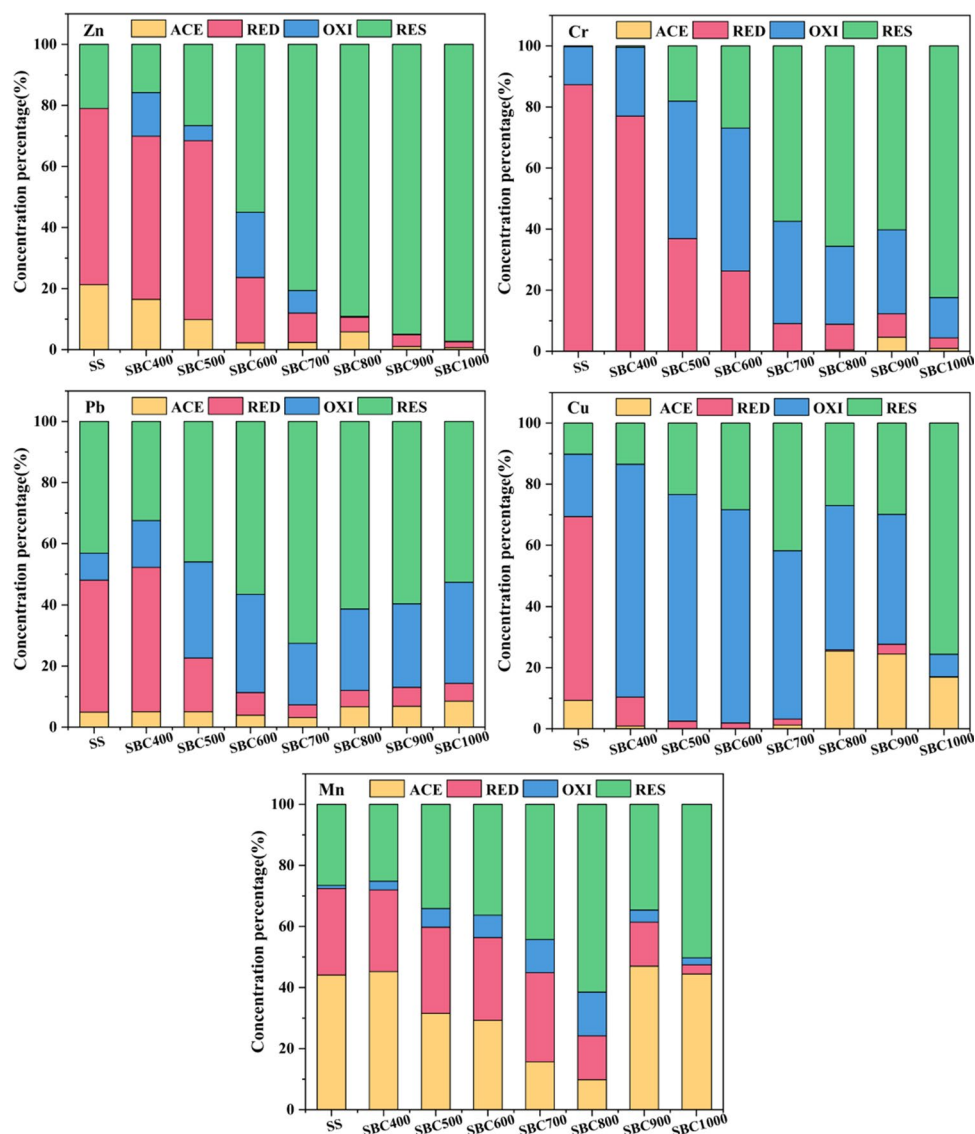
FTIR analysis, revealing that pyrolysis temperature changes the properties of sludge biochar.

Effect of pyrolysis temperature on heavy metal bioavailability and ecological risk

Heavy metal bioavailability

The concentration of heavy metals in SS and SBC is shown in Table S2. As the pyrolysis temperature increased, the percentage of heavy metals in SBC increased due to the decomposition of organic matters (Hossain et al. 2011). The concentrations of heavy metals in the SS and SBC followed the sequence of $\text{Zn} > \text{Cu} > \text{Mn} > \text{Cr} > \text{Pb}$, which was consistent with previous research (Lu et al. 2015; Zhang et al. 2020b). The concentration of Zn was much higher than those of other heavy metals, which may be related to the extensive use of galvanized pipes in China (Jin et al. 2016). As seen from Fig. 2, the heavy metals in SS were mainly ACE and RED, which had higher bioavailability and mobility. With

Fig. 2 Heavy metals (Zn, Cr, Pb, Cu, Mn) fraction distribution in the SS and SBC



the increase of pyrolysis temperature, the proportion of more stabilized OXI and RES increased, revealing that pyrolysis can significantly immobilize heavy metals in the SS. At pyrolysis temperature above 800 °C, the OXI and RES content of Cu and Mn decreased, probably because of the release and volatilization of Cu and Zn due to the decomposition of carbonate and silicate (Li et al. 2018a).

Ecological risk assessment of heavy metals in SS and SBC

Figure S2 and Fig. 3 show the ecological risk indexes of SS and SBC. For SS, Cr had the highest ecological risk factor E_r among the five heavy metals investigated, and the potential ecological risk index RI reached up to 787.0, suggesting the high ecological risk due to the existence of heavy metals. RI decreased to 491.6 after pyrolysis at 400 °C and significantly

decreased to low risk above 500 °C. As a result, pyrolysis at temperature above 500 °C is suggested in order to immobilize and decrease the ecological risk of heavy metals in SS.

Influencing factors on Cd(II) adsorption

The Pseudo-first-order and Pseudo-second-order kinetics modeling are shown in Fig. 4a. The adsorption capacity of Cd(II) by SBC increased rapidly within 5 h due to the large number of accessible adsorption sites. The adsorption occurred at the outer surface of SBC and was mainly controlled by diffusion (Kołodziejńska et al. 2012; Ni et al. 2019). The adsorption reached equilibrium thereafter due to the saturation of the active adsorption site. Table 2 shows the fitting parameters of adsorption kinetics curve. The best fitting was provided by the Pseudo-second-order model

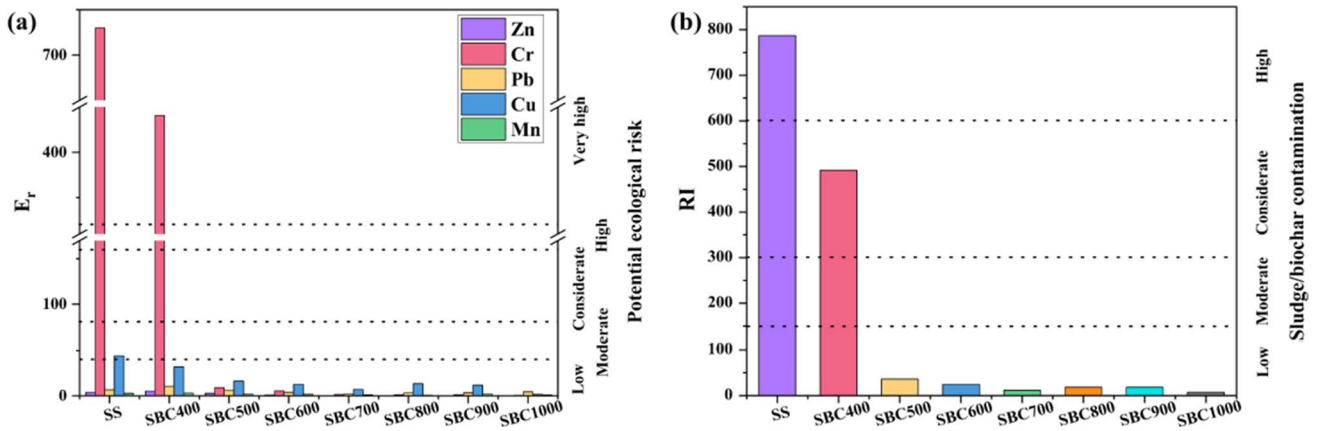


Fig. 3 a The potential ecological risk factor of individual heavy metals; b the potential ecological risk index of the SS and sludge biochar

Fig. 4 Effect of a pyrolysis temperature, b initial pH, c coexisting cations and anions on Cd(II) adsorption by SBC. In figure b, c, and d, the initial Cd(II) concentration was 50 ppm and the SBC700 dosage was 0.40 g·L⁻¹

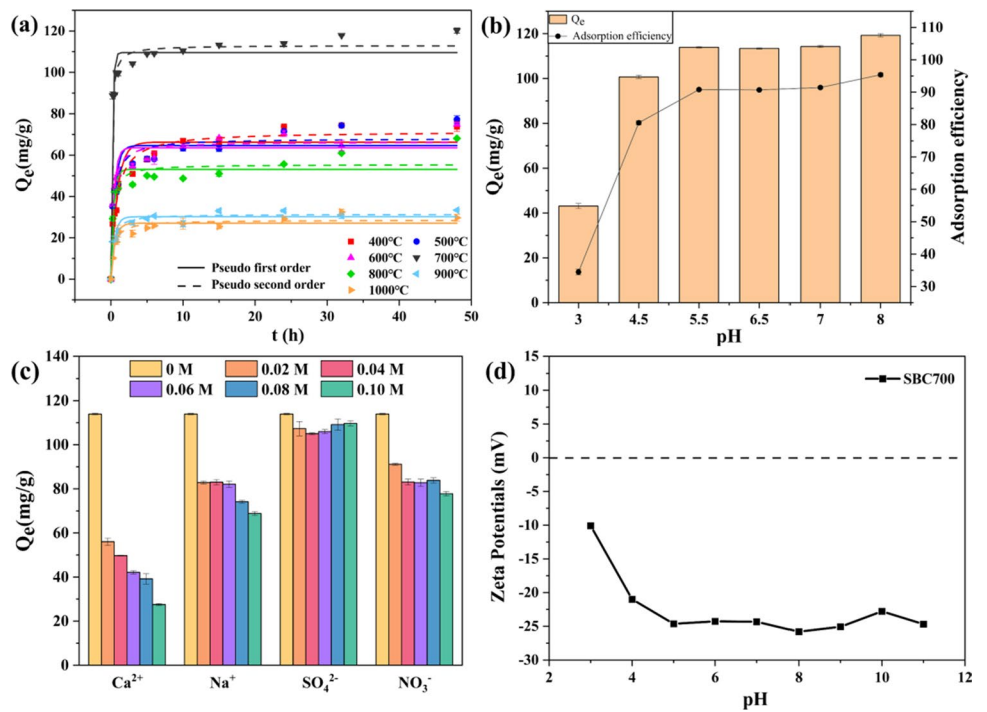


Table 2 Pseudo-first-order and Pseudo-second-order model parameters for Cd(II) adsorption by SBC obtained under different pyrolysis temperatures (400–1000 °C)

Sample	Pseudo-first-order kinetic model			Pseudo-second-order kinetic model		
	Q_e (mg·g ⁻¹)	k_1 (h ⁻¹)	R_1^2	Q_e (mg·g ⁻¹)	k_2 [(g·h) ⁻¹]	R_2^2
SBC400	66.23	1.1307	0.8961	71.47	0.0202	0.9601
SBC500	64.63	1.8304	0.8453	68.11	0.0401	0.9210
SBC600	63.53	2.6752	0.8909	66.40	0.0575	0.9463
SBC700	109.60	5.2007	0.9414	110.06	0.0938	0.9795
SBC800	53.12	2.7105	0.8487	55.51	0.0790	0.8935
SBC900	30.19	2.0025	0.8811	31.43	0.1078	0.9418
SBC1000	27.04	1.8063	0.9046	28.57	0.0896	0.9379

($R_1^2 < R_2^2$), implying that chemical mechanism played an important role in Cd(II) adsorption (Chen et al. 2021; Fan et al. 2017). SBC700 had the highest adsorption capacity with the maximum adsorption capacity at $120.24 \text{ mg}\cdot\text{g}^{-1}$, which was related to its highest specific surface area and more abundant oxygen-containing functional groups. The maximum adsorption capacity is comparable to most of the modified biochar. Besides, the minimum ecological risk and maximum adsorption capacity can be achieved simultaneously at 700°C . Therefore, SBC700 was utilized to investigate the effect of pH and co-existing ions.

Figure 4b shows the effect of initial pH on Cd(II) adsorption by SBC700. The adsorption capacity was the lowest at pH 3.0 due to the competition of H^+ with Cd(II) for the adsorption sites. The adsorption capacity increased with pH increasing from 3.0 to 5.5, which was consistent with the result of Li et al. (2017). The deprotonation of carboxylic and hydroxyl functional groups increased the negative charges on the surface of SBC with the increase of pH, and then the number of binding sites increased (Khan et al. 2020a). Meanwhile, the concentration of H^+ decreased with the increase of pH, which made it less competitive (Usman et al. 2016). At pH 8, the removal capacity increased, probably due to the precipitation of Cd(II) at alkaline pH.

The effect of coexisting cations and anions on Cd(II) adsorption by SBC700 is shown in Fig. 4c. Both of the existence of Ca^{2+} and Na^+ inhibited the adsorption of Cd(II) and Ca^{2+} was severely interfere with the adsorption, which was consistent with the result of Zhao et al. (2020). The main reason was that Ca^{2+} had a stronger covalent nature, so it was more competitive to adsorb Cd(II) (Wang et al. 2018). SO_4^{2-} almost had no effect on Cd(II) adsorption, but NO_3^- inhibited the Cd(II) adsorption. This was because the ability of monovalent anion to compete for the active center of adsorbent was stronger than that of Cd(II), and the increase of its concentration will reduce the probability of collision between Cd(II) and adsorbent (Zhao et al., 2020). However, due to the negative charge on the surface of SBC700 (Fig. 4d), it was more difficult for SO_4^{2-} to approach SBC700 than NO_3^- , so the inhibition of SO_4^{2-} was not obvious. Besides, Ca^{2+} released into the solution by ion exchange inhibited Cd(II) adsorption (Fan et al. 2017), while SO_4^{2-} formed insoluble CaSO_4 ($\text{pK}_{\text{sp}} = 5.04$) with Ca^{2+} , which counteracted the inhibition of both ions. The inhibition of coexisting ions Ca^{2+} , Na^+ , and NO_3^- on Cd(II) adsorption enhanced with the increase of concentration.

Adsorption mechanism

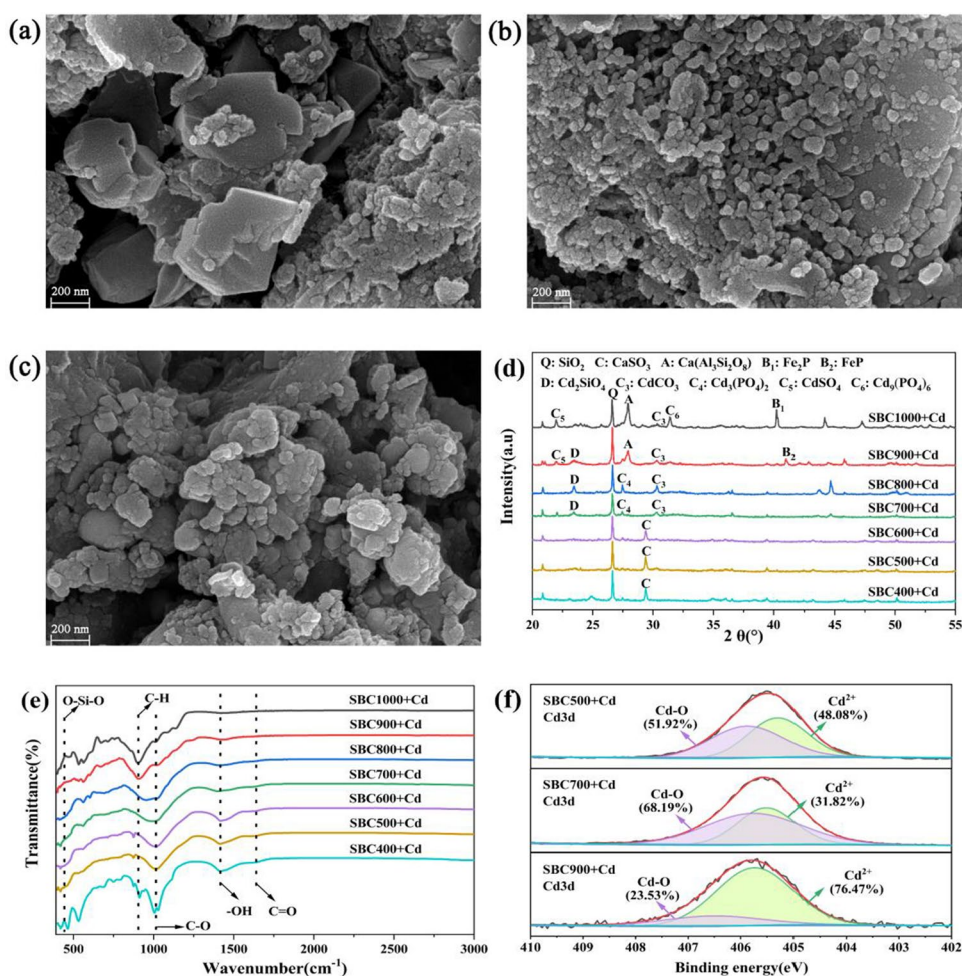
The SEM images of SBC500, SBC700, and SBC900 after Cd(II) adsorption are shown in Fig. 5. Many spherical nanoparticles with particles size at 40–80 nm adhered to the SBC surface and pores, indicating that Cd precipitate

was formed at the surface of SBC (Wu et al. 2021). Combined with EDS analysis (Fig. S3), it was found that the content of Cd increased, suggesting that Cd(II) was successfully adsorbed. SEM images showed that the adsorption of Cd(II) on SBC500 was concentrated in the pores, while it was observed both at the surface and pores on SBC700, this was consistent with the result of higher adsorption capacity of SBC700 in adsorption kinetics. Due to the obvious reduction of pores caused by sintering at high temperature, the adsorption of SBC900 mainly occurred at the surface. Besides, Ca content dropped sharply in the EDS image of SBC500 after adsorption. Ca^{2+} in solution was thought to be released from SBC after Cd(II) adsorption (Fan et al. 2017), so it was speculated that SBC500 adsorbed Cd(II) through ion exchange.

The XRD spectrum of sludge biochar after Cd(II) adsorption is shown in Fig. 5d. No obvious differences were observed in the XRD spectrum of SBC before and after Cd(II) adsorption at pyrolysis temperature at $400\text{--}600^\circ\text{C}$, indicating that the precipitates containing Cd(II) were predominantly in the form of amorphous compounds (Chen et al. 2015). The characteristic peaks corresponding to CdSO_4 , Cd_2SiO_4 , $\text{Cd}_3(\text{PO}_4)_2$, CdCO_3 , and $\text{Cd}_9(\text{PO}_4)_6$ appeared at high temperature ($700\text{--}1000^\circ\text{C}$) (Zama et al. 2017), suggesting that the removal of Cd(II) was mainly through the interaction of Cd(II) and minerals to form surface precipitates (Gao et al. 2019). Besides, the characteristic peaks corresponding to CaS disappeared after adsorption, speculating that CaS was involved in the adsorption process. The increase of pyrolysis temperature will change the mineral composition of biochar and produce anions such as SO_4^{2-} , SiO_4^{4-} , PO_4^{3-} , and CO_3^{2-} (Qiu et al. 2021). As can be seen from Fig. 5d, the number of characteristic peaks increased with the increase of pyrolysis temperature, indicating that the contribution of co-precipitation increased.

Some characteristic peaks of the SBC in the FTIR spectrum after Cd(II) adsorption shifted (Fig. 5e). For example, the peak at 866 cm^{-1} , 1037 cm^{-1} , 1420 cm^{-1} , and 1615 cm^{-1} , corresponding to C-H, C-O, -OH, and C=O, shifted to 886 cm^{-1} , 1051 cm^{-1} , 1433 cm^{-1} , and 1643 cm^{-1} , respectively. This indicated that these functional groups were involved in the binding of SBC and Cd(II) through cation- π interaction, surface complexation and ion exchange (Fan et al. 2017). The change of C-H indicated that aromatic functional groups such as $\gamma\text{-CH}$ of furan contributed to the adsorption by providing π electrons; the coordination of Cd^{2+} with π electrons was beneficial to the adsorption of Cd(II) by SBC (Gao et al. 2019). In addition, C-O, -OH, and C=O peaks weakened at lower pyrolysis temperature, suggesting that -COOH and -OH oxygen-containing functional groups were more involved in the reaction by complexation (Fan et al., 2017).

Fig. 5 SEM images of **a** SBC500, **b** SBC700, and **c** SBC900 after Cd(II) adsorption; **d** FTIR spectrum of seven sludge biochar after Cd(II) adsorption; **e** XRD spectrum of seven sludge biochar after Cd(II) adsorption; **f** Cd3d narrow scan spectra of SBC500, SBC700, and SBC900 after Cd(II) adsorption



The wide scan XPS spectrum of SBC500, SBC700, and SBC900 after adsorption (Fig. S4a) shows the existence of Cd, conforming that Cd(II) was successfully adsorbed on SBC. The new CO_3^{2-} and Cd–O peaks appeared in the C1s (Fig. S4b) and O1s (Fig. S4c) narrow scan spectra indicated that Cd(II) may form CdCO_3 precipitate and be adsorbed on the surface of biochar (Chen et al. 2021; Yuan et al. 2020). The Cd^{2+} and Cd–O peaks appeared in the Cd3d narrow scan spectrum (Fig. 5f); related studies had confirmed that their occurrence corresponded to the mechanism of ion exchange and complexation, respectively (Zhang et al. 2015; Khan et al. 2020b). The difference of the peak area of Cd^{2+} and Cd–O in the three kinds of sludge biochar resulted in the difference of adsorption mechanism. The effect of ion exchange and complexation was comparable in SBC500, and it was consistent with SEM analysis and characterization of more oxygen-containing functional groups. The peak area of Cd–O in SBC700 was more than twice that of Cd^{2+} , indicating that SBC700 was dominated by complexation, which consistent with the fact that SBC700 had the highest peak area of C=O in XPS characterization. Some of the oxygen-containing functional groups decomposed on

the surface of SBC900 while the number of exchangeable cations increased at high temperature. The peak area of Cd^{2+} in SBC900 was significantly higher than that of Cd–O; ion exchange was its main adsorption mechanism. Figure 6 summarizes the main adsorption mechanism of Cd(II) by SBC.

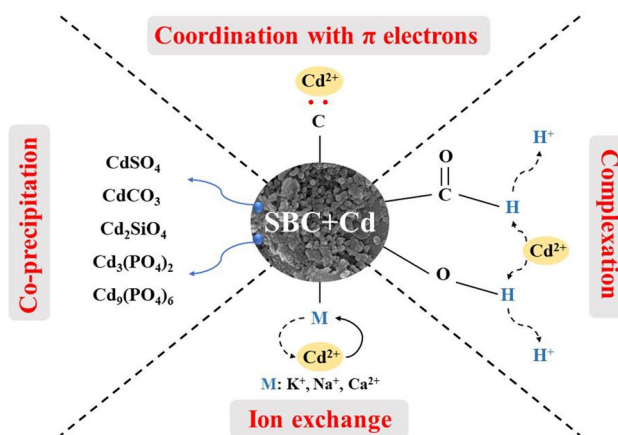


Fig. 6 The main adsorption mechanism of Cd(II) by SBC

Conclusion

Through the characterization of SBC, it was found that surface functional groups of SBCs were changed by pyrolysis. The content of C-H increased with the increase of pyrolysis temperature, while oxygen-containing functional groups such as C-O, -OH, and C=O were reduced. The proportion of more stabilized OXI and RES in SBC increased with the pyrolysis temperature increased; however, ACE content of Cu and Mn increased at temperature above 800 °C. The ecological risk of heavy metals in SS decreased with the increase of pyrolysis temperature, and it decreased to low risk above 500 °C in general. The Cd(II) adsorption mechanism of SBC mainly included co-precipitation with SO_4^{2-} , SiO_4^{4-} , PO_4^{3-} , and CO_3^{2-} coordination with π electrons and ion exchange with K^+ , Na^+ , and Ca^{2+} . The complexation of SBC was significant at 400–700 °C, but its contribution decreased with the decrease of surface functional groups at high pyrolysis temperature. The practical application conditions of SBC are complex, so it is necessary to further study its adsorption performance in the presence of other heavy metals. In addition, due to the interaction of natural factors, the long-term risk of SBC in the natural environment needs further investigation.

Supplementary Information The online version contains supplementary material available at <https://doi.org/10.1007/s11356-022-22827-x>.

Author contribution Methodology: Menglan Wu, Bo Liu; Investigation: Menglan Wu, Bo Liu; Data curation: Menglan Wu, Bo Liu; Visualization: Menglan Wu, Bo Liu; Writing - original draft: Menglan Wu; Writing - review & editing: Menglan Wu, Bo Liu, Jun Li, Xintai Su, Weizhen Liu, Xiaoqin Li; Funding acquisition: Xintai Su, Weizhen Liu, Xiaoqin Li; Conceptualization: Xiaoqin Li; Supervision: Xiaoqin Li.

Funding This work was supported by the National Key Research and Development Program of China (No. 2019YFA0210401), the National Natural Science Foundation of China (No. 21836002), and the Guangdong Science and Technology Program, China (2020B121201003).

Data availability The data used and/or analyzed during the current study are available.

Declarations

Ethical approval Not applicable.

Consent to participate Not applicable.

Consent for publication Not applicable.

Competing interests The authors declare no competing interests.

References

Carolin CF, Kumar PS, Saravanan A, Joshiba GJ, Naushad M (2017) Efficient techniques for the removal of toxic heavy metals from

aquatic environment: a review. *J Environ Chem Eng* 5:2782–2799. <https://doi.org/10.1016/j.jece.2017.05.029>

- Chen T, Zhang Y, Wang H, Lu W, Zhou Z, Zhang Y, Ren L (2014) Influence of pyrolysis temperature on characteristics and heavy metal adsorptive performance of biochar derived from municipal sewage sludge. *Bioresour Technol* 164:47–54. <https://doi.org/10.1016/j.biortech.2014.04.048>
- Chen T, Zhou Z, Han R, Meng R, Wang H, Lu W (2015) Adsorption of cadmium by biochar derived from municipal sewage sludge: impact factors and adsorption mechanism. *Chemosphere* 134:286–293. <https://doi.org/10.1016/j.chemosphere.2015.04.052>
- Chen Y, Li M, Li Y, Liu Y, Chen Y, Li H, Li L, Xu F, Jiang H, Chen L (2021) Hydroxyapatite modified sludge-based biochar for the adsorption of Cu(2+) and Cd(2+): adsorption behavior and mechanisms. *Bioresour Technol* 321:124413. <https://doi.org/10.1016/j.biortech.2020.124413>
- Fan S, Li H, Wang Y, Wang Z, Tang J, Tang J, Li X (2017) Cadmium removal from aqueous solution by biochar obtained by copyrolysis of sewage sludge with tea waste. *Res Chem Intermed* 44:135–154. <https://doi.org/10.1007/s11164-017-3094-1>
- Gao LY, Deng JH, Huang GF, Li K, Cai KZ, Liu Y, Huang F (2019) Relative distribution of Cd(2+) adsorption mechanisms on biochars derived from rice straw and sewage sludge. *Bioresour Technol* 272:114–122. <https://doi.org/10.1016/j.biortech.2018.09.138>
- Gu S, Kang X, Wang L, Lichtfouse E, Wang C (2018) Clay mineral adsorbents for heavy metal removal from wastewater: a review. *Environ Chem Lett* 17:629–654. <https://doi.org/10.1007/s10311-018-0813-9>
- Hossain MK, Strezov V, Chan KY, Ziolkowski A, Nelson PF (2011) Influence of pyrolysis temperature on production and nutrient properties of wastewater sludge biochar. *J Environ Manage* 92:223–228. <https://doi.org/10.1016/j.jenvman.2010.09.008>
- Huang Y, He C, Shen C, Guo J, Mubeen S, Yuan J, Yang Z (2017) Toxicity of cadmium and its health risks from leafy vegetable consumption. *Food Funct* 8:1373–1401. <https://doi.org/10.1039/c6fo01580h>
- Jin J, Li Y, Zhang J, Wu S, Cao Y, Liang P, Zhang J, Wong MH, Wang M, Shan S, Christie P (2016) Influence of pyrolysis temperature on properties and environmental safety of heavy metals in biochars derived from municipal sewage sludge. *J Hazard Mater* 320:417–426. <https://doi.org/10.1016/j.jhazmat.2016.08.050>
- Khan ZH, Gao M, Qiu W, Islam MS, Song Z (2020a) Mechanisms for cadmium adsorption by magnetic biochar composites in an aqueous solution. *Chemosphere* 246:125701. <https://doi.org/10.1016/j.chemosphere.2019.125701>
- Khan ZH, Gao M, Qiu W, Song Z (2020b) Properties and adsorption mechanism of magnetic biochar modified with molybdenum disulfide for cadmium in aqueous solution. *Chemosphere* 255:126995. <https://doi.org/10.1016/j.chemosphere.2020.126995>
- Kołodziejka D, Krukowska J, Thomas P (2017) Comparison of sorption and desorption studies of heavy metal ions from biochar and commercial active carbon. *Chem Eng J* 307:353–363. <https://doi.org/10.1016/j.cej.2016.08.088>
- Kołodziejka D, Wnętrzak R, Leahy JJ, Hayes MHB, Kwapiński W, Hubicki Z (2012) Kinetic and adsorptive characterization of biochar in metal ions removal. *Chem Eng J* 197:295–305. <https://doi.org/10.1016/j.cej.2012.05.025>
- LI B, DING S, FAN H. & REN Y. 2021. Experimental investigation into the effect of pyrolysis on chemical forms of heavy metals in sewage sludge biochar (SSB), with brief ecological risk assessment. *Materials (Basel)*, 14. <https://doi.org/10.3390/ma14020447>
- Li B, Yang L, Wang CQ, Zhang QP, Liu QC, Li YD, Xiao R (2017) Adsorption of Cd(II) from aqueous solutions by rape straw biochar derived from different modification processes. *Chemosphere* 175:332–340. <https://doi.org/10.1016/j.chemosphere.2017.02.061>

- Li S, Harris S, Anandhi A, Chen G (2019) Predicting biochar properties and functions based on feedstock and pyrolysis temperature: a review and data syntheses. *J Clean Prod* 215:890–902. <https://doi.org/10.1016/j.jclepro.2019.01.106>
- Li Z, Deng H, Yang L, Zhang G, Li Y, Ren Y (2018a) Influence of potassium hydroxide activation on characteristics and environmental risk of heavy metals in chars derived from municipal sewage sludge. *Bioresour Technol* 256:216–223. <https://doi.org/10.1016/j.biortech.2018.02.013>
- Li Z, Wang L, Meng J, Liu X, Xu J, Wang F, Brookes P (2018b) Zeolite-supported nanoscale zero-valent iron: new findings on simultaneous adsorption of Cd(II), Pb(II), and As(III) in aqueous solution and soil. *J Hazard Mater* 344:1–11. <https://doi.org/10.1016/j.jhazmat.2017.09.036>
- Liang L, Li X, Guo Y, Lin Z, Su X, Liu B (2021) The removal of heavy metal cations by sulfidated nanoscale zero-valent iron (S-nZVI): the reaction mechanisms and the role of sulfur. *J Hazard Mater* 404:124057. <https://doi.org/10.1016/j.jhazmat.2020.124057>
- LIANG, L., LI, X., LIN, Z., TIAN, C. & GUO, Y. 2020. The removal of Cd by sulfidated nanoscale zero-valent iron: the structural, chemical bonding evolution and the reaction kinetics. *Chem Eng J*, 382. <https://doi.org/10.1016/j.cej.2019.122933>
- Liu L, Huang L, Huang R, Lin H, Wang D (2021) Immobilization of heavy metals in biochar derived from co-pyrolysis of sewage sludge and calcium sulfate. *J Hazard Mater* 403:123648. <https://doi.org/10.1016/j.jhazmat.2020.123648>
- Lu T, Yuan H, Wang Y, Huang H, Chen Y (2015) Characteristic of heavy metals in biochar derived from sewage sludge. *J Mater Cycles Waste Manage* 18:725–733. <https://doi.org/10.1007/s10163-015-0366-y>
- Ni BJ, Huang QS, Wang C, Ni TY, Sun J, Wei W (2019) Competitive adsorption of heavy metals in aqueous solution onto biochar derived from anaerobically digested sludge. *Chemosphere* 219:351–357. <https://doi.org/10.1016/j.chemosphere.2018.12.053>
- QIU B, TAO X, WANG H, LI W, DING X. & CHU H. 2021. Biochar as a low-cost adsorbent for aqueous heavy metal removal: a review. *J Anal App Pyrolysis*, 155. <https://doi.org/10.1016/j.jaap.2021.105081>
- USMAN A, SALLAM A, ZHANG M, VITHANAGE M, AHMAD M, AL-FARRAJ A, OK YS, ABDULJABBAR A. & AL-WABEL M. 2016. Sorption process of date palm biochar for aqueous Cd (II) removal: efficiency and mechanisms. *Water Air Soil Poll*, 227. <https://doi.org/10.1007/s11270-016-3161-z>
- Wang S, Kwak JH, Islam MS, Naeth MA, GAMAL EL-DIN, M. & CHANG, S. X. (2020) Biochar surface complexation and Ni(II), Cu(II), and Cd(II) adsorption in aqueous solutions depend on feedstock type. *Sci Total Environ* 712:136538. <https://doi.org/10.1016/j.scitotenv.2020.136538>
- Wang X, Li C, Li Z, Yu G, Wang Y (2019) Effect of pyrolysis temperature on characteristics, chemical speciation and risk evaluation of heavy metals in biochar derived from textile dyeing sludge. *Ecotoxicol Environ Saf* 168:45–52. <https://doi.org/10.1016/j.ecoenv.2018.10.022>
- Wang Y-Y, Liu Y-X, Lu H-H, Yang R-Q, Yang S-M (2018) Competitive adsorption of Pb(II), Cu(II), and Zn(II) ions onto hydroxyapatite-biochar nanocomposite in aqueous solutions. *J Solid State Chem* 261:53–61. <https://doi.org/10.1016/j.jssc.2018.02.010>
- Wu J, Wang T, Wang J, Zhang Y, Pan WP (2021) A novel modified method for the efficient removal of Pb and Cd from wastewater by biochar: enhanced the ion exchange and precipitation capacity. *Sci Total Environ* 754:142150. <https://doi.org/10.1016/j.scitotenv.2020.142150>
- Xiong Q, Wu X, Lv H, Liu S, Hou H, Wu X (2021) Influence of rice husk addition on phosphorus fractions and heavy metals risk of biochar derived from sewage sludge. *Chemosphere* 280:130566. <https://doi.org/10.1016/j.chemosphere.2021.130566>
- Xue Y, Wang C, Hu Z, Zhou Y, Xiao Y, Wang T (2019) Pyrolysis of sewage sludge by electromagnetic induction: biochar properties and application in adsorption removal of Pb(II), Cd(II) from aqueous solution. *Waste Manag* 89:48–56. <https://doi.org/10.1016/j.wasman.2019.03.047>
- Yoon K, Cho DW, Tsang DCW, Bolan N, Rinklebe J, Song H (2017) Fabrication of engineered biochar from paper mill sludge and its application into removal of arsenic and cadmium in acidic water. *Bioresour Technol* 246:69–75. <https://doi.org/10.1016/j.biortech.2017.07.020>
- Yuan S, Hong M, Li H, Ye Z, Gong H, Zhang J, Huang Q, Tan Z (2020) Contributions and mechanisms of components in modified biochar to adsorb cadmium in aqueous solution. *Sci Total Environ* 733:139320. <https://doi.org/10.1016/j.scitotenv.2020.139320>
- Yuan X, Huang H, Zeng G, Li H, Wang J, Zhou C, Zhu H, Pei X, Liu Z, Liu Z (2011) Total concentrations and chemical speciation of heavy metals in liquefaction residues of sewage sludge. *Bioresour Technol* 102:4104–4110. <https://doi.org/10.1016/j.biortech.2010.12.055>
- Zama EF, Zhu Y-G, Reid BJ, Sun G-X (2017) The role of biochar properties in influencing the sorption and desorption of Pb(II), Cd(II) and As(III) in aqueous solution. *J Clean Prod* 148:127–136. <https://doi.org/10.1016/j.jclepro.2017.01.125>
- Zhang F, Wang X, Yin D, Peng B, Tan C, Liu Y, Tan X, Wu S (2015) Efficiency and mechanisms of Cd removal from aqueous solution by biochar derived from water hyacinth (*Eichornia crassipes*). *J Environ Manage* 153:68–73. <https://doi.org/10.1016/j.jenvman.2015.01.043>
- Zhang J, Jin J, Wang M, Naidu R, Liu Y, Man YB, Liang X, Wong MH, Christie P, Zhang Y, Song C, Shan S (2020a) Co-pyrolysis of sewage sludge and rice husk/ bamboo sawdust for biochar with high aromaticity and low metal mobility. *Environ Res* 191:110034. <https://doi.org/10.1016/j.envres.2020.110034>
- Zhang P, Li Y, Cao Y, Han L (2019) Characteristics of tetracycline adsorption by cow manure biochar prepared at different pyrolysis temperatures. *Bioresour Technol* 285:121348. <https://doi.org/10.1016/j.biortech.2019.121348>
- ZHANG Q, YE X, LI H, CHEN D, XIAO W, ZHAO S, XIONG R. & LI J. 2020b. Cumulative effects of pyrolysis temperature and process on properties, chemical speciation, and environmental risks of heavy metals in magnetic biochar derived from coagulation-flocculation sludge of swine wastewater. *Journal of Environmental Chemical Engineering*, 8. <https://doi.org/10.1016/j.jece.2020.104472>
- Zhang X, Zhang P, Yuan X, Li Y, Han L (2020c) Effect of pyrolysis temperature and correlation analysis on the yield and physico-chemical properties of crop residue biochar. *Bioresour Technol* 296:122318. <https://doi.org/10.1016/j.biortech.2019.122318>
- Zhao B, Xu X, Liu W, Zhang R, Cui M, Liu J, Zhang W (2021) The evaluation of immobilization behavior and potential ecological risk of heavy metals in bio-char with different alkaline activation. *Environ Sci Pollut Res Int* 28:21396–21410. <https://doi.org/10.1007/s11356-020-12183-z>
- Zhao N, Li B, Huang H, Lv X, Zhang M, Cao L (2020) Modification of kelp and sludge biochar by TMT-102 and NaOH for cadmium adsorption. *J Taiwan Inst Chem Eng* 116:101–111. <https://doi.org/10.1016/j.jtice.2020.10.036>

Publisher's note Springer Nature remains neutral with regard to jurisdictional claims in published maps and institutional affiliations.

Springer Nature or its licensor holds exclusive rights to this article under a publishing agreement with the author(s) or other rightsholder(s); author self-archiving of the accepted manuscript version of this article is solely governed by the terms of such publishing agreement and applicable law.